

Pressure lineshift and broadening coefficient of H₂O by hydrogen and helium in the 1.39 μm region with a tunable diode laser spectrometer

V. Zéninari,¹ B. Parvite,¹ D. Courtois,¹ I. Pouchetm,²
G. Durry,² and Yu.N. Ponomarev³

¹ *Groupe de Spectrométrie Moléculaire et Atmosphérique, UMR CNRS 6089, UFR Sciences Exactes et Naturelles, Reims, Cedex 2, France*

² *Service d'Aéronomie du CNRS, CNRS-Réduit de Verrières, Verrières-le-Buisson Cedex, France*

³ *Institute of Atmospheric Optics, Siberian Branch of the Russian Academy of Sciences, Tomsk, Russia*

Received January 10, 2003

A near-infrared diode laser spectrometer was used in the laboratory to measure H₂O line strengths and shifts by H₂ and He pressure near 1.39 μm. Hydrogen and helium broadened halfwidths and shifts of water vapor have been measured for some 5 transitions. These lines from the $\nu_1 + \nu_3$ and $2\nu_1$ bands were selected either because they are used for the "Spectromètre à diodes lasers" SDLA spectrometer or to complete a set of lines with different J parameters for isolated and quite strong lines.

Introduction

To measure the concentrations of minor gaseous constituents (for example, H₂O) in the atmospheres of giant planets from atmospheric IR spectra, it is necessary to know the regularities of transformation of spectral line profiles of the studied gas by the pressure of H₂ and He, which are the dominant constituents of the atmospheres of giant planets.

The data for molecular absorption line parameters of H₂O are contained in relevant databases, e.g., in HITRAN,¹ but in the shortwave spectral region corresponding to wavelengths shorter than 1.5 μm, the data on strengths and halfwidth for many lines are not sufficiently accurate, while the data on pressure induced shifts (even for air) are often lacking.

The region of 1.39 μm covered by the radiation of the diode laser operating at the room temperature is promising for development of high-sensitivity gas analyzers or lidars for sensing of spatial H₂O concentration profiles. In the previous paper² we have reported precision measurements of H₂O intensities near 1.39 μm conducted with the high-resolution diode laser spectrometer and shown that the data from the HITRAN database in this region was sometimes far from our measured parameters, while our experimental results were closer to the *ab initio* calculations of Partridge and Schwenke.³

While the line strengths and energy levels are now relatively well known, the pressure broadening halfwidths have major uncertainties and pressure induced lineshifts are sometimes unknown. For the atmospheres of giant planets, such as Jupiter, the broadening of H₂O absorption lines by H₂ and He

pressure must be known. The effects of errors in the halfwidth on the retrieved H₂O vertical profiles have been investigated with the conclusion that inaccurate collision-broadened halfwidth values lead to significant errors in the retrieved profiles.⁴

Hydrogen and helium broadened halfwidths of water vapor have been measured here for some 5 transitions. These lines from the $\nu_1 + \nu_3$ and $2\nu_1$ bands were selected because they are used for the "Spectromètre à diodes lasers" (SDLA) spectrometer⁵ – a near infrared diode laser spectrometer for the *in situ* measurements of CH₄ and H₂O from stratospheric balloons. We also report here hydrogen and helium lineshift coefficients.

Experimental details

The H₂O absorption spectra are recorded at high resolution in the laboratory with a tunable diode laser (TDL) spectrometer. Our experimental arrangement is schematically shown in Fig. 1. The laser source is a fiber-coupled distributed feedback (DFB) InGaAs diode laser that has been developed for the SDLA experiment by THALES – France. It exhibits high performance: the average output power is 10 mW, the laser linewidth < 10 MHz and there are no mode-hops in the tunability range. The continuous tuning range (at constant temperature) is > 3 cm⁻¹. This point is of particular interest for our experiments where the maximum pressure may be 1330 mbar and the collisional line broadening is important.

The diode includes a Faraday optical isolator to prevent optical feedback and emits at 7180 cm⁻¹ at room temperature with the maximum power of

12 mW while the temperature and current tuning rates are, respectively, $0.09 \text{ nm} \cdot ^\circ\text{C}^{-1}$ and $0.0078 \text{ nm} \cdot \text{mA}^{-1}$.

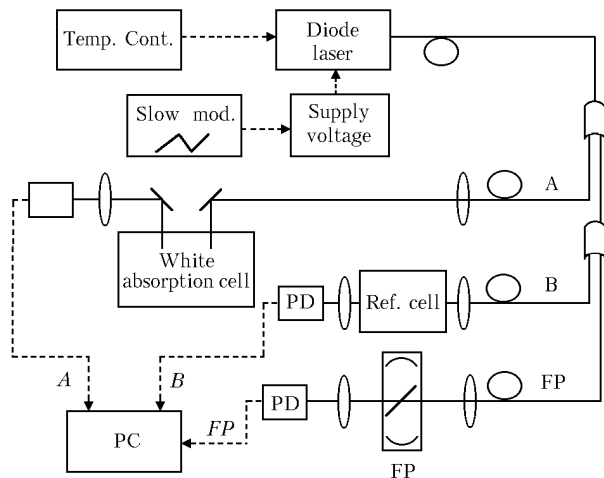


Fig. 1. Scheme of the absorption spectrometer. Temp. Cont. stands for temperature controller, Slow mod. stands for slow modulation, PD stands for photodiode, Ref. cell stands for reference cell, and FP stands for Fabry–Perot interferometer.

The laser wavelength is temperature stabilized by means of a Peltier element and is driven by a low noise current supply. A low-frequency ramp at 100 Hz is used to scan the DFB diode over the selected absorption lines by modulation of the driving current.

The pigtailed laser diode mounted in an emission module is junctioned to a second 50/50 fused coupler. The main beam (A) is collimated and passed through an absorption White-type cell. The remaining part of the beam is junctioned to a second 50/50 fused coupler. One beam is collimated and coupled with a confocal Fabry–Perot (FP) interferometer used for frequency calibration (free spectral range 0.0095 cm^{-1}). The other beam passes through the reference cell (B). The whole set-up takes place in a closed box, filled with dry nitrogen at atmospheric pressure in order to minimize the absorption by ambient water vapor. Furthermore, the use of optical fibers to conduct light and the use of fused couplers instead of beam splitters is convenient to prevent further corruption by ambient H_2O over the optical path followed by the laser beam. The three signals A, B, and FP are sent to a digital oscilloscope and to a personal computer for data acquisition (10 ms per spectrum, 11 bit resolution).

We use two different absorption cells for this study: a small (10 cm long) cylindrical Pyrex cell for the reference (B) and a multiple path White-type cell (A) with a path length adjustable between 1 and 10 meters.⁶ For broadening and shift coefficients measurements the White cell is filled with pure water at low pressure and completed with high purity (99.9995%) gases helium and hydrogen from Air Liquide – France. The reference cell is filled with

5 mbar of pure water vapor. The pressure is measured with an uncertainty of 0.5% using two MKS Baratron manometers with 10 and 1000 Torr full scale. All measurements are done at room temperature ($296 \pm 1 \text{ K}$).

We record numerous spectra for each pressure varying from 6 to 1330 mbar for the five lines under study. Figure 2 presents an example of one recorded spectrum ($660 \leftarrow 661$ transition of the $\nu_1 + \nu_3$ band of H_2O at $7185.5960 \text{ cm}^{-1}$) with increasing pressure of hydrogen. One should remark the increasing linewidth and the pressure lineshift on the left (negative shift). The Fabry–Perot interferometer fringes are also presented.

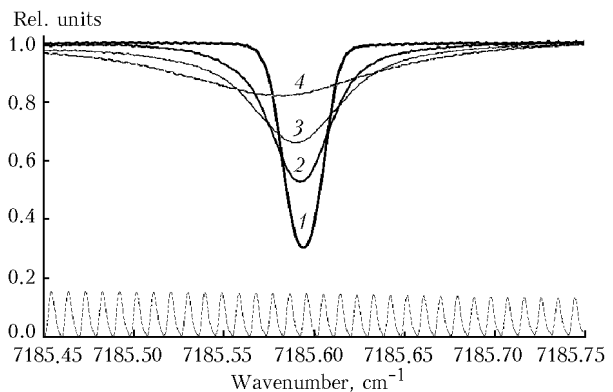


Fig. 2. Example of recorded spectra for the $660 \leftarrow 661$ of the $\nu_1 + \nu_3$ band of H_2O at $7185.5960 \text{ cm}^{-1}$ with increasing pressure of H_2 . The Fabry–Perot interferometer fringes are shown at the bottom.

Data inversion

To retrieve the broadening coefficients and lineshifts, we fit a Voigt profile to the molecular transmission. The molecular transmission $\hat{O}(\sigma)$ is obtained from the 3 recorded signals A, B, and FP in two steps. First the FP signal is used to retrieve the frequency variation law by a five-degree polynomial interpolation on the interferences fringes. In the second step the method used to retrieve the molecular transmission $\hat{O}(\sigma)$ is from the direct absorption signals A or B using $\hat{A} = \hat{A}_0 \hat{O}(\sigma)$ (\hat{A}_0 is what would be the laser flux in the absence of absorber in the cell). \hat{A}_0 is obtained from A by a five-degree polynomial interpolation over full transmission region. The line intensity $S(T)$ is related to the molecular transmission through the Beer–Lambert law

$$T(\sigma) = I_T(\sigma)/I_0(\sigma) = \exp[-k(\sigma, \theta, P) l],$$

where l is the optical path length, and the absorption coefficient $k(\sigma, \theta, P)$ at temperature θ and for a gas pressure P is modeled using the Voigt profile

$$k(\sigma, \theta, P) = S(\theta) A \frac{y}{\pi} \int_{-\infty}^{+\infty} \frac{\exp(-t^2)}{y^2 + (x-t)^2} dt, \quad (1)$$

$$A = \frac{\sqrt{\ln 2}}{\gamma_D \sqrt{\pi}}; \quad y = \sqrt{\ln 2} \frac{\gamma_{\text{col}}}{\gamma_D}; \quad x = \sqrt{\ln 2} \frac{(\sigma - \sigma_0)}{\gamma_D}, \quad (2)$$

where $S(\theta)$ is the line intensity at temperature θ , σ_0 is the line center wavenumber at pressure P , γ_D is the Doppler halfwidth, and γ_{col} is the collisional halfwidth, $\gamma_{\text{col}} = \gamma_{\text{self}} P c + \gamma_0 P(1 - c)$; γ_{self} is the self-broadening coefficient obtained from Toth,⁷ c is the concentration of H₂O molecules, and γ_0 is the broadening coefficient for the studied perturbing gas (hydrogen or helium).

The Voigt profile cannot be expressed in analytical form but may be expressed as the real part of the complex probability function $W(x, y)$ defined by

$$W(x, y) = \frac{i}{\pi} \int_{-\infty}^{+\infty} \frac{\exp(-t^2)}{x + iy - t} dt, \quad (3)$$

which can be evaluated using the Humlicek algorithm.⁸

We check that the apparatus function of the spectrometer was negligible by recording low pressure (< 0.05 mbar) spectra. Under these conditions the lineshape could be fitted by a simple Gaussian curve having a Doppler width in good agreement with the theoretical value. One example of recorded spectrum for the $101 \leftarrow 110$ transition of the $2\nu_1$ band of H₂O at $7182.2091 \text{ cm}^{-1}$ is presented in Fig. 3 with the fitted Voigt profile and the residual.

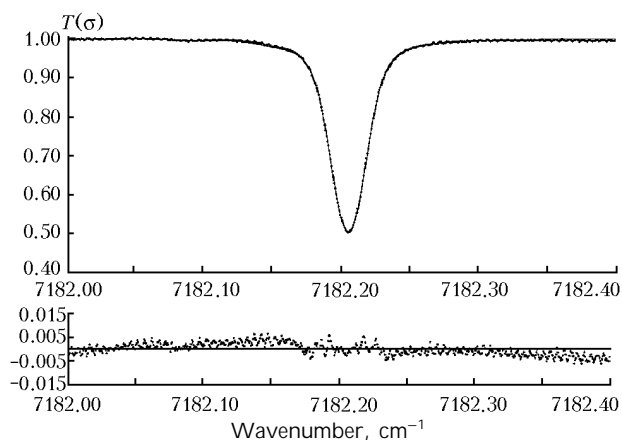


Fig. 3. Example of recorded spectra for the $101 \leftarrow 110$ transition of the $2\nu_1$ band of H₂O at $7182.2091 \text{ cm}^{-1}$. Experimental profiles (dots) and fitted Voigt profile (solid curve) are presented. The (observed minus calculated) residuals are shown at the bottom.

Voigt and Rautian⁹ profiles were tried with similar results. The Rautian profile gives systematically slightly higher results of collisional widths at low pressure but the slopes of the straight lines obtained by plotting γ_0 vs. p are comparable.

The collisional lineshift $\delta = \sigma_0(\text{H}_2\text{O-perturber}) - \sigma_0(\text{H}_2\text{O})$ is obtained by subtracting the peak frequency of the pressure broadened line from that of the reference line. As these spectra are simultaneously recorded, the accuracy of the shift depends on the

linearity and relative calibration of the wavenumber scale but is independent of determination of the absolute wavenumber of the lines. For every chosen line and perturber, the measured shifts are plotted against the total pressure and are fitted to a straight line in order to determine the shift coefficient δ_0 in $\text{cm}^{-1} \cdot \text{atm}^{-1}$.

Experimental results and conclusion

The intensity of the five studied lines is reported in Table 1. Uncertainties are reported in %. The complete set of H₂O transitions lying within the tuning range of the THALES laser diode is reported in Ref. 2. The results in this paper are carefully compared with previous determinations and available databases.

Table 1. Absolute line intensities for the five selected lines of H₂O

Transition $J' K'_a K'_c \leftarrow J K_a K_c$	Band	σ_0 , cm^{-1}	S_0 , cm^{-1}	Uncer- tainty, %
			molec. $\cdot\text{cm}^{-2}$	
1 0 1 \leftarrow 1 1 0	$2\nu_1$	7182.2091	$1.52 \cdot 10^{-21}$	2
2 1 2 \leftarrow 3 1 3	$\nu_1 + \nu_3$	7182.94935	$3.69 \cdot 10^{-21}$	2
3 0 3 \leftarrow 3 2 2	$\nu_1 + \nu_3$	7175.98675	$2.59 \cdot 10^{-22}$	2
5 1 5 \leftarrow 5 1 4	$\nu_1 + \nu_3$	7165.21504	$6.27 \cdot 10^{-22}$	2
6 6 0 \leftarrow 6 6 1*	$\nu_1 + \nu_3$	7185.5960	$7.85 \cdot 10^{-22}$	2

* This line is in fact an unresolved doublet. The strength given here corresponds to the sum of the strengths of the 2 lines. The rotational quantum assignment given corresponds to the stronger transition.

Figure 4 presents an example of the pressure dependence of the collisional halfwidth for the $212 \leftarrow 313$ line of the $\nu_1 + \nu_3$ band of H₂O at $7182.94955 \text{ cm}^{-1}$ perturbed by H₂ and He. Figure 5 presents the pressure dependence of the lineshift for the same line and perturbers.

The slope of the best fit lines represents the collisional halfwidth and lineshift coefficients. For some lines the maximal pressure for the calculation of the slope was only 600 mbar due to strong close lines. Table 2 shows the experimental values for the halfwidth and lineshift coefficients expressed in $\text{cm}^{-1} \cdot \text{atm}^{-1}$ along with the estimated global errors.

These uncertainties are the sum of the statistical errors derived from the linear fit. The absolute wavenumbers are from Ref. 10. One should make the following remarks:

The broadening coefficient by He is approximately three times smaller than that by H₂. It decreases with the J quantum number and is two times smaller for the line with $J = 6$ regarding to the other lines.

The lineshift coefficient by H₂ is always negative. Its absolute value increases a little for $J = 1$ to $J = 3$ and then decreases.

The lineshift coefficient by He seems to have the same comportment with increasing J but in this case the shift is almost always positive. It decreases a little for $J = 1$ to $J = 3$ and then increases.

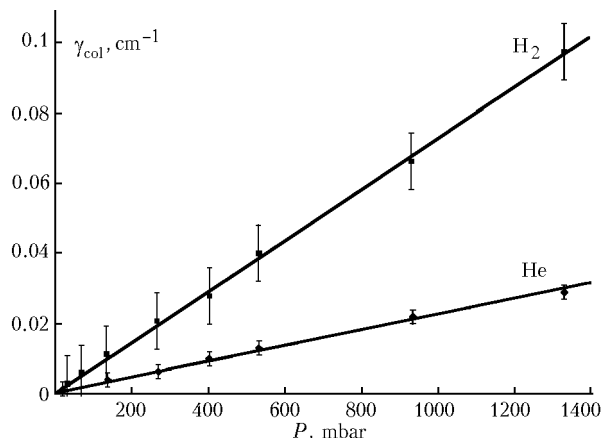


Fig. 4. Pressure dependence of the collisional halfwidth for the $2\ 1\ 2 \leftarrow 3\ 1\ 3$ line of the $\nu_1 + \nu_3$ band of H_2O at $7182.94955\ \text{cm}^{-1}$ perturbed by H_2 and He .

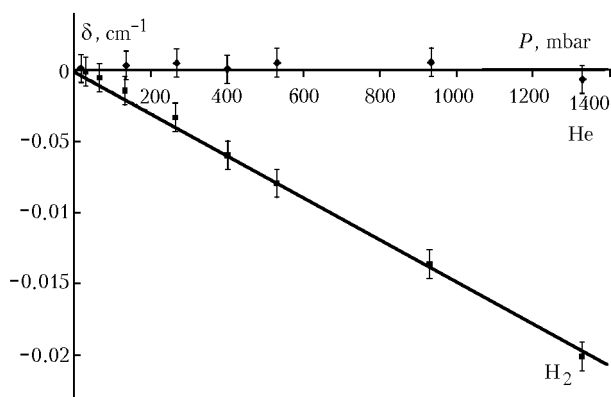


Fig. 5. Pressure dependence of the collisional lineshift for the $2\ 1\ 2 \leftarrow 3\ 1\ 3$ line of the $\nu_1 + \nu_3$ band of H_2O at $7182.94955\ \text{cm}^{-1}$ perturbed by H_2 and He .

Table 2. H_2 and He broadening γ_0 and shift δ_0 coefficients of H_2O absorption lines in $\text{cm}^{-1}\cdot\text{atm}^{-1}$

Transition $J' K'_a K'_c \leftarrow J K_a K_c$	Band	σ_0, cm^{-1}	$\gamma_0 (\text{H}_2)$	$\delta_0 (\text{H}_2)$	$\gamma_0 (\text{He})$	$\delta_0 (\text{He})$
1 0 1 \leftarrow 1 1 0	$2\nu_1$	7182.2091	0.084 ± 0.008	-0.014 ± 0.001	0.023 ± 0.002	0.002 ± 0.001
2 1 2 \leftarrow 3 1 3	$\nu_1 + \nu_3$	7182.94955	0.073 ± 0.008	-0.015 ± 0.001	0.023 ± 0.002	0.000 ± 0.001
3 0 3 \leftarrow 3 2 2	$\nu_1 + \nu_3$	7175.98675	0.077 ± 0.008	-0.015 ± 0.001	0.027 ± 0.003	-0.001 ± 0.001
5 1 5 \leftarrow 5 1 4	$\nu_1 + \nu_3$	7165.21504	0.069 ± 0.008	-0.012 ± 0.001	0.022 ± 0.003	0.0023 ± 0.0006
6 6 0 \leftarrow 6 6 1	$\nu_1 + \nu_3$	7185.5960	0.043 ± 0.004	-0.010 ± 0.001	0.012 ± 0.001	0.006 ± 0.001

Theoretical estimation of the broadening and lineshift coefficients for $| \bar{2} \bar{1} \bar{1} \rangle - | \bar{2} \bar{2} \bar{1} \rangle$ collisions with allowance for the major contribution of the dipole-quadrupole interaction by the model from Ref. 11 yields the mean (for the studied lines) value of the broadening coefficient equal to $0.035\ \text{cm}^{-1}\cdot\text{atm}^{-1}$ and that of the lineshift coefficient equal to $0.005\ \text{cm}^{-1}\cdot\text{atm}^{-1}$. These estimates are obtained without using experimental data in the fitting procedure and, therefore, they are approximate. The components of the polarizability tensor of the $| \bar{2} \bar{2} \bar{1} \rangle$ molecule obtained from processing of the data on argon pressure induced lineshifts for the $| \bar{2} \bar{2} \bar{1} \rangle \nu_2 + \nu_3$, which may differ considerably from the components of the polarizability tensor for the $\nu_1 + \nu_3$ state were taken into account as well.

These experimental results will be compared with theoretical calculations in collaboration with the Institute of Atmospheric Optics.

Acknowledgments

This laboratory work was supported by the Programme National de Chimie Atmosphérique of the Institut National des Sciences de l'Univers (INSU) of the Centre National de la Recherche Scientifique (CNRS – France).

References

1. L.S. Rothman, C.P. Rinsland, A. Goldman, S.T. Massie, D.P. Edwards, J.-M. Flaud, A. Perrin, C. Camy-Peyret, V. Dana, J.-Y. Mandin, J. Schroeder, A. McCann, R.R. Gamache, R.B. Wattson, K. Yoshino, K.V. Chance,

- K.W. Jucks, L.R. Brown, V. Nemtchinov, and P. Varanasi, *The HITRAN molecular spectroscopic database and HAWKS (HITRAN atmospheric workstation): 1996 Edition*, *J. Quant. Spectrosc. Radiat. Transfer* **60**, 665 (1998).
2. B. Parvitte, V. Zeninari, I. Pouchet, and G. Durré, *Diode laser spectroscopy of H_2O in the 7165–7185 cm^{-1} range for atmospheric applications*, *J. Quant. Spectrosc. Radiat. Transfer* **75**, 493 (2002).
3. H. Partridge, D.W. Schwenke, *The determination of an accurate isotope dependent potential energy surface for water from extensive ab initio calculations and experimental data*, *J. Chem. Phys.* **106**, 4618 (1997).
4. R.R. Gamache, R. Lynch, and L.R. Brown, *Theoretical calculations of pressure broadening coefficients for H_2O perturbed by hydrogen and helium gas*, *J. Quant. Spectrosc. Radiat. Transfer* **56**, 471 (1996).
5. G. Durré and I. Pouchet, *A near-infrared diode laser spectrometer for the in situ measurements of CH_4 and H_2O from stratospheric balloons*, *J. Atmos. Ocean. Tech.* **1**, 1485 (2001).
6. D. Courtois, A. Delahaigie, C. Thiébeaux, H. Le Corre, and J.C. Mouanda, *Adjustable-temperature and multiple-path optical cell for ozone spectroscopy*, *J. Phys. E: Sci. Instrum.* **21**, 863 (1988).
7. R.A. Toth, L.R. Brown, and C. Plymate, *Self-broadened widths and frequency shifts of water vapor lines between 590 and 2400 cm^{-1}* , *J. Quant. Spectrosc. Radiat. Transfer* **59**, 529 (1998).
8. J. Humlicek, *Optimized computation of the Voigt and complex probability functions*, *J. Quant. Spectrosc. Radiat. Transfer* **27**, 437 (1982).
9. S.G. Rautian and Sobel'man, *Sov. Phys. Usp.* **9**, 701 (1967).
10. R.A. Toth, *Extensive measurements of H_2O line frequencies and strengths in 5750 to 7965 cm^{-1}* , *Appl. Opt.* **33**, 4851 (1994).